

The Full Spectrum of Deep Net Hessians At Scale: Dynamics with Sample Size

Vardan Papyan
Stanford University
Stanford CA 94305, USA
papyan@stanford.edu

Abstract

Previous works observed the spectrum of the Hessian of the training loss of deep neural networks. However, the networks considered were of minuscule size. We apply state-of-the-art tools in modern high-dimensional numerical linear algebra to approximate the spectrum of the Hessian of deep nets with tens of millions of parameters. Our results corroborate previous findings, based on small-scale networks, that the Hessian exhibits ‘spiked’ behavior, with several outliers isolated from a continuous bulk. However we find that the bulk does not follow a simple Marchenko-Pastur distribution, as previously suggested, but rather a heavier-tailed distribution. Finally, we document the dynamics of the outliers and the bulk with varying sample size.

1. Introduction

We consider the task of image classification, where we are given a set of images $\{x_{\text{train}}^i\}_{i=1}^{n_{\text{train}}}$ and their corresponding labels $\{y_{\text{train}}^i\}_{i=1}^{n_{\text{train}}}$ and our task is to predict the labels on future data $\{x_{\text{test}}^i, y_{\text{test}}^i\}_{i=1}^{n_{\text{test}}}$. State-of-the-art methods tackle this problem using deep convolutional neural networks. Those are trained by minimizing the empirical cross-entropy loss ℓ on the training data,

$$\mathcal{L}(\theta) = \text{Ave}_{\text{train}} \{\ell_{\text{train}}^i(\theta)\}, \quad (1)$$

where $\ell_{\text{train}}^i(\theta) = \ell(f(x_{\text{train}}^i; \theta), y_{\text{train}}^i)$ and $\text{Ave}_{\text{train}}$ is the operator that averages n_{train} elements. Here we denoted by $f(x_{\text{train}}^i; \theta) \in \mathbb{R}^C$ the output of the classifier and by $\theta \in \mathbb{R}^p$ the concatenation of all the parameters in the network into a single vector.

In this work we investigate two Hessians: the Hessian of the loss averaged over the training data and the testing data

$$H_{\text{train}}(\theta) = \text{Ave}_{\text{train}} \{\nabla^2 \ell_{\text{train}}^i(\theta)\} \quad (2)$$

$$H_{\text{test}}(\theta) = \text{Ave}_{\text{test}} \{\nabla^2 \ell_{\text{test}}^i(\theta)\}, \quad (3)$$

where $\ell_{\text{test}}^i(\theta) = \ell(f(x_{\text{test}}^i; \theta), y_{\text{test}}^i)$ and Ave_{test} is the operator that averages n_{test} elements. The former can be seen

as an empirical approximation of the the Fisher information matrix – a quantity that is of utmost interest in the analysis of the generalization properties of estimators; while the latter measures variation in the test loss that would be caused by perturbations in the model and is therefore also of significant importance. Following the ideas presented in [14], we use the Gauss-Newton decomposition of the train (and similarly test) Hessian and write it as a summation of two components:

$$H_{\text{train}}(\theta) = \underbrace{\text{Ave}_{\text{train}} \left\{ \ell_{\text{train}}^i{}'(\theta) \nabla^2 f(x_{\text{train}}^i; \theta) \right\}}_{\text{averaged Hessian of predictions}} \quad (4) \\ + \underbrace{\text{Ave}_{\text{train}} \left\{ \ell_{\text{train}}^i{}''(\theta) \nabla f(x_{\text{train}}^i; \theta) \nabla f(x_{\text{train}}^i; \theta)^T \right\}}_{\text{covariance of gradients}},$$

where

$$\ell_{\text{train}}^i{}'(\theta) = \ell'(f(x_{\text{train}}^i; \theta), y_{\text{train}}^i) \quad (5)$$

$$\ell_{\text{train}}^i{}''(\theta) = \ell''(f(x_{\text{train}}^i; \theta), y_{\text{train}}^i). \quad (6)$$

Pioneering work by Sagun et al. [14, 15] introduced the study of the train Hessian and made some initial numerical studies and some initial interpretations on small-scale networks. They presented histograms of the eigenvalues of the Hessian and observed visually that the histogram exhibited a bulk together with a few large outliers. They further observed that the number of such outliers is often equal to the number of classes in the classification problem. Their claim was that the bulk is affected by the architecture while the outliers depend on the data. Leaning further on a random matrix theory analogy, the authors further suggested that the bulk might be modeled as a Marchenko-Pastur (MP) distribution [11].

Certain observed properties of deepnet Hessian spectra are qualitatively similar to those seen in the theory of covariance estimation in modern high-dimensional statistics, where they arise under the so-called spiked covariance model [7]. Much is known about its properties [2, 3, 13] and it is therefore of interest to know whether it indeed models the spectrum of the Hessian faithfully.

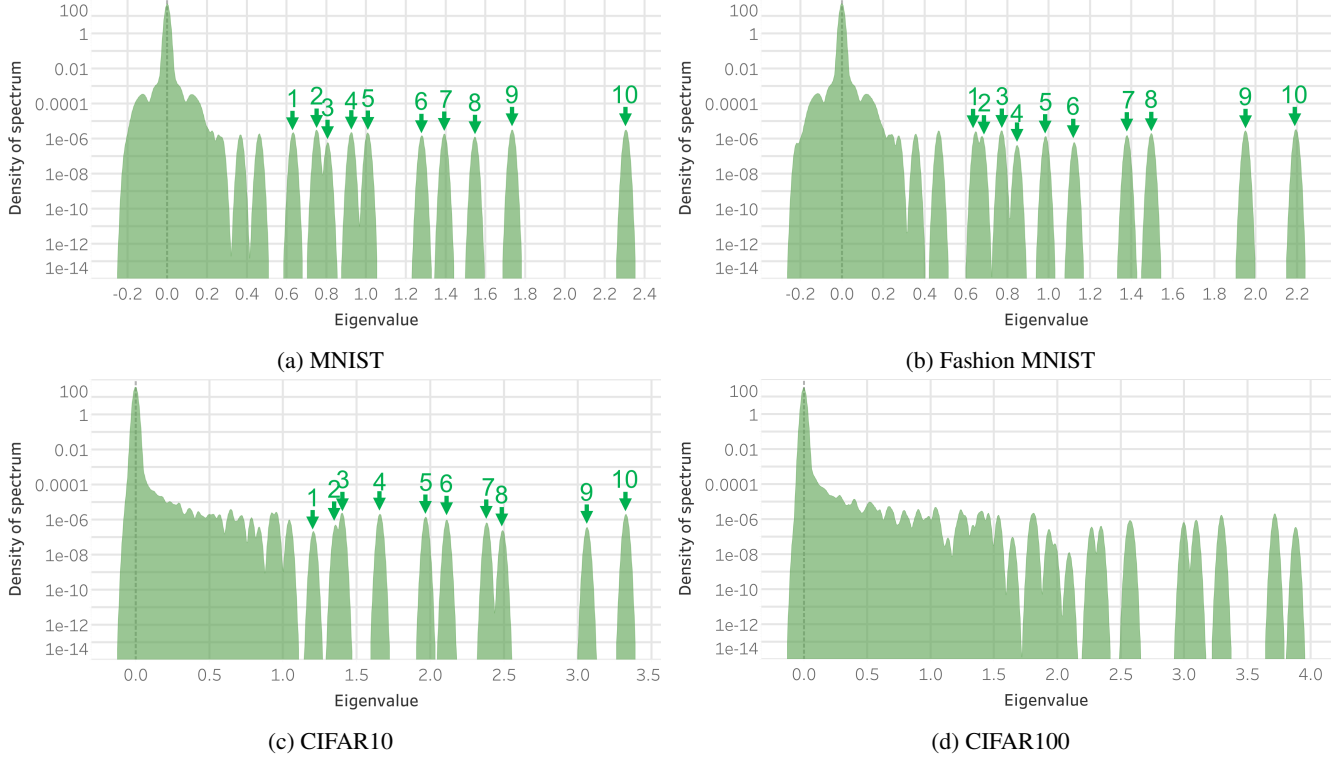


Figure 1: *Spectrum of the **train** Hessian for VGG11 trained on various datasets.* Panels (a)-(d) document famous datasets in Deep Learning. In all cases there is a big concentration of eigenvalues at zero due to the large number of parameters in the model (28 million) compared to the small amount of training examples (50 thousand). In MNIST, Fashion MNIST and CIFAR10 we observe a clear bulk-and-outliers structure. The number of outliers arguably corresponds to the number of classes and there exists a clear separation of the outliers from the bulk. In CIFAR100 the situation is more complicated. Some of the outliers are clearly separated from the bulk, while others are less clearly evident. One possibly sees traces ‘buried’ inside the bulk. However, their number is very large, making their distinction harder to draw. As pointed out by [14, 15], negative eigenvalues exist in the spectrum of the train Hessian. This is despite the fact that the model was trained for hundreds of epochs, the learning rate was annealed twice and its initial value was optimized over a large set of values.

In [14, 15] the authors inaugurated the empirical study of spectral properties of deepnet Hessians. However, their exploration was limited to architectures with **thousands** of parameters – orders of magnitude smaller than state-of-the-art architectures such as VGG [16] and ResNet [6] that have **tens of millions** of parameters. Our first contribution in this work is to leverage state-of-the-art tools in numerical linear algebra to approximate the spectrum of the Hessian of networks such as VGG and ResNet. As a teaser for what is to come, Figures 1 and 2 show the train and test Hessian of VGG11 – an architecture with 28 millions of parameters – on various known datasets.

Our second contribution is to confirm previous reports of bulk-and-outliers structure, this time *at the full scale of modern state-of-the-art nets*. We find that the bulk-and-outliers structure indeed manifests itself across *many different datasets, networks and control parameters*, as can be seen from Figures 1 and 2.

The authors of [14, 15] focused on smaller-scale Hessians as a whole and not on the two components: the covariance of the gradients and the averaged Hessian of predictions. Our third and fourth contributions, on the other hand, relate to their individual analysis.

Our third contribution is the study of the covariance of the gradients. This term is defined as the outer product of i.i.d gradients. Moreover, our experiments show its spectrum contains outliers and a small but non-negligible bulk. These outliers can be tracked throughout different sample sizes and are therefore fundamental components, whereas the bulk is sporadic and changes from one scenario to the next. Based on these findings, a potential theoretical model for the covariance of the gradients is the spiked covariance model [7] or its generalized version [1].

Our fourth contribution is the study of the averaged Hessian of predictions. We observe that its spectrum does not contain outliers; thereby we can solidly *attribute the out-*

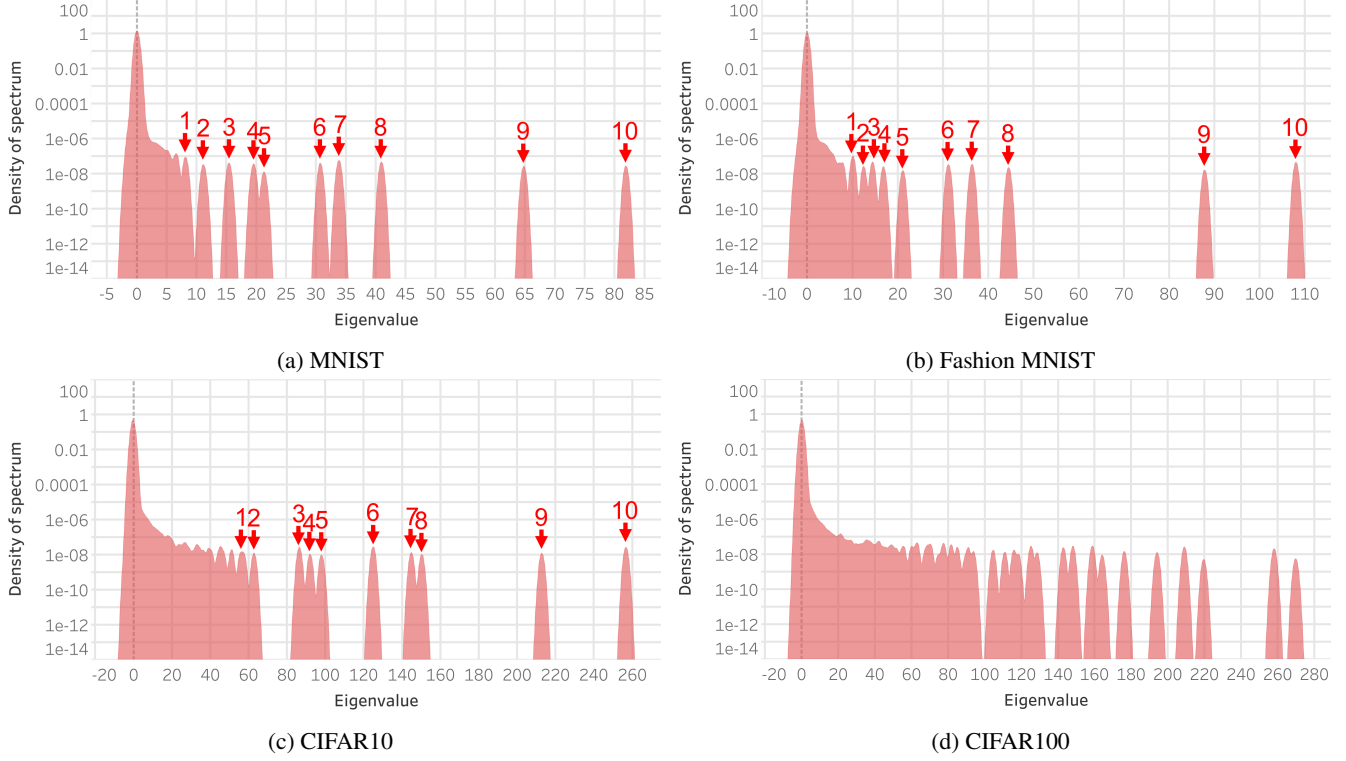


Figure 2: *Spectrum of the **test** Hessian for VGG11 trained on various datasets.* Panels (a)-(d) document famous datasets in Deep Learning. In all cases there is a big concentration of eigenvalues at zero due to the large number of parameters in the model (28 million) compared to the small amount of testing examples (10 thousand). Similar to the train Hessian; in MNIST, Fashion MNIST and CIFAR10 we observe a clear bulk-and-outliers structure, where the number of outliers arguably corresponds to the number of classes. Contrary to the train Hessian, some of the outliers are less clearly evident, although one possibly sees traces ‘buried’ just inside the upper bulk. In CIFAR100 the situation is again more complicated due to the large amount of outliers. Note there is a clear difference in magnitude between the train and test Hessian (despite the fact that both were normalized by the number of contributing terms).

liers of the Hessian to the covariance of the gradients. We observe that most of the energy in the bulk of the spectrum can be attributed to the averaged Hessian of predictions. We also observe that the bulk of the Hessian *does not* follow a Marcenko-Pastur distribution, contrary to previous suggestion. This complements recent empirical observations [12] that the spectrum of the *trained weights* in deep neural networks follows a heavy-tailed distribution.

In future work we plan to model the scaling of generalization errors of deep nets as function of sample size using spectral properties of deepnet Hessians. As preparation, our fifth contribution is the analysis of *both the train and test Hessians across varying sample size*. We explore the dynamics of the outliers and the bulk with varying amounts of train data, showing a clear separation of the outliers (signals) from the bulk (noise) with increased sample size.

We summarize below our main deliverables:

- We provide an algorithm that allows to approximate

the spectrum of the Hessian of deep nets with tens of millions of parameters.

- We study the behavior of spectral properties of deep-net Hessians, both the train and test, across different datasets, networks and control parameters.
- We analyze not only the spectrum of the Hessian but also its two components, the covariance of the gradients and the averaged Hessian of predictions.
- We attribute the outliers of the Hessian to the covariance of the gradients component.
- We observe that most of the energy in the bulk of the spectrum can be attributed to the averaged Hessian of predictions, which does not follow a MP distribution.
- We investigate the dynamics of the outliers and the bulk with varying sample size.

2. Tools from numerical linear algebra

Our approach for approximating the Hessian of deep nets builds on the survey of [10], which discussed several different methods for approximating the density of the spectrum of large linear operators; many of these were first developed in the context of studies of large linear operators in quantum mechanics by physicists and chemists starting from the 1970's [5, 18, 17, 4]. From the methods presented therein, we implemented and tested two: the Lanczos method and the Kernel Polynomial Method (KPM). From our experience the Lanczos method was effective and useful, while KPM was temperamental and in some ways problematic. As such, we focus on Lanczos in this work, but provide an implementation for both in our released software.

2.1. SLOWLANCZOS

The Lanczos algorithm [8] computes the spectrum of a symmetric matrix $H \in \mathbb{R}^{p \times p}$ by first reducing it to a tridiagonal form $T_p \in \mathbb{R}^{p \times p}$ and then computing the spectrum of that matrix instead. The motivation is that computing the spectrum of a tridiagonal matrix is very efficient, requiring only $O(p)$ operations. The algorithm works by progressively building an adapted orthonormal basis $V_m \in \mathbb{R}^{p \times m}$ that satisfies at each iteration the relation

$$V_m^T H V_m = T_m, \quad (7)$$

where $T_m \in \mathbb{R}^{m \times m}$ is a tridiagonal matrix. For completeness, we summarize its main steps in Algorithm 1.

2.2. Complexity of SLOWLANCZOS

We start with the runtime complexity and assume without loss of generality that we are computing the spectrum of the train Hessian. Each of the p iterations of the algorithm requires a single Hessian-vector multiplication $H_{\text{train}}(\theta)v_m$. Since

$$H_{\text{train}}(\theta)v_m = \text{Ave}_{\text{train}} \{ \nabla^2 \ell_{\text{train}}^i(\theta)v_m \}, \quad (8)$$

computing this product requires iterating through a dataset of size n_{train} once. In each iteration the Hessian of a single example $\nabla^2 \ell_{\text{train}}^i(\theta)$ is multiplied by the vector v_m , incurring $O(p)$ complexity, where p is the number of parameters in the model. The complexity due to all Hessian-vector multiplications is therefore $O(n_{\text{train}}p^2)$. The m 'th iteration also requires a reorthogonalization step, which computes the inner product of m vectors of length p and costs $O(mp)$ complexity. Summing this over the iterations, $m = 1, \dots, p$, the complexity incurred due to reorthogonalization is $O(p^3)$. The total runtime complexity of the algorithm is therefore $O(n_{\text{train}}p^2 + p^3)$. As for memory requirements, the algorithm constructs a basis $V_p \in \mathbb{R}^{p \times p}$ and as such its memory complexity is $O(p^2)$. Since p is in the order of magnitude of tens of millions, both time and memory complexity make SLOWLANCZOS impractical.

Algorithm 1: SLOWLANCZOS(H)

Input: Linear operator $H \in \mathbb{R}^{p \times p}$.

Result: Exact spectrum of H .

for $m = 1, \dots, p$ **do**

if $m == 1$ **then**

 sample $v \sim \mathcal{N}(0, I)$;

$v_1 = \frac{v}{\|v\|_2}$;

$w = H v_1$;

else

$w = H v_m - \beta_{m-1} v_{m-1}$;

end

$\alpha_m = v_m^T w$;

$w = w - \alpha_m v_m$;

 /* reorthogonalization

*/

$w = w - V_m V_m^T w$;

$\beta_m = \|w\|_2$;

$v_{m+1} = \frac{w}{\beta_m}$;

end

$$T_p = \begin{bmatrix} \alpha_1 & \beta_1 & & & \\ \beta_1 & \alpha_2 & \beta_2 & & \\ & \beta_2 & \alpha_3 & & \\ & & & \ddots & \beta_{p-1} \\ & & & \beta_{p-1} & \alpha_p \end{bmatrix};$$

$\{\theta_m\}_{m=1}^p, \{y_m\}_{m=1}^p = \text{eig}(T_p)$;

return $\{\theta_m\}_{m=1}^p, \{y_m\}_{m=1}^p$;

2.3. Spectral density estimation via FASTLANCZOS

As a first step towards making Lanczos suitable for the problem we attack in this paper, we remove the reorthogonalization step in Algorithm 1. This allows us to save only three terms $-v_{\text{prev}}, v$ and v_{next} instead of the whole matrix $V_m \in \mathbb{R}^{p \times m}$ (see Algorithm 2). This greatly reduces the memory complexity of the algorithm at the cost of a nuisance that is discussed in Section 2.5. Moreover, it removes the $O(p^3)$ term from the runtime complexity.

In light of the runtime complexity analysis in the previous subsection, it is clear that running Lanczos for p iterations is impractical. Realizing that, the authors of [10] proposed to run the algorithm for $M \ll p$ iterations and compute an approximation to the spectrum based on the eigenvalues $\{\theta_m\}_{m=1}^M$ and eigenvectors $\{y_m\}_{m=1}^M$ of T_M . Denoting by τ_m the first element in y_m , their proposed approximation was

$$\phi(t) = \sum_{m=1}^M \tau_m^2 \delta(t - \theta_m), \quad (9)$$

where δ is the Dirac delta function. They further proposed to improve the approximation by starting the algorithm from several different starting vectors, $v_1^l, l = 1, \dots, n_{\text{vec}}$, and

Algorithm 2: FASTLANCZOS(H, M)

Input: Linear operator $H \in \mathbb{R}^{p \times p}$ with spectrum in the range $[-1, 1]$.
Number of iterations M .

Result: Eigenvalues and eigenvectors of the tridiagonal matrix T_M .

for $m = 1, \dots, M$ **do**

if $m == 1$ **then**

 sample $v \sim \mathcal{N}(0, I)$;

$v = \frac{v}{\|v\|_2}$;

$v_{\text{next}} = Hv$;

else

$v_{\text{next}} = Hv - \beta_{m-1}v_{\text{prev}}$;

end

$\alpha_m = v_{\text{next}}^T v$;

$v_{\text{next}} = v_{\text{next}} - \alpha_m v$;

$\beta_m = \|v_{\text{next}}\|_2$;

$v_{\text{next}} = \frac{v_{\text{next}}}{\beta_m}$;

$v_{\text{prev}} = v$;

$v = v_{\text{next}}$;

end

$$T_M = \begin{bmatrix} \alpha_1 & \beta_1 & & & \\ \beta_1 & \alpha_2 & \beta_2 & & \\ & \beta_2 & \alpha_3 & & \\ & & & \ddots & \beta_{M-1} \\ & & & \beta_{M-1} & \alpha_M \end{bmatrix};$$

$\{\theta_m\}_{m=1}^M, \{y_m\}_{m=1}^M = \text{eig}(T_M)$;

return $\{\theta_m\}_{m=1}^M, \{y_m\}_{m=1}^M$;

averaging the results as follows

$$\phi(t) = \frac{1}{n_{\text{vec}}} \sum_{l=1}^{n_{\text{vec}}} \sum_{m=1}^M \tau_m^l{}^2 \delta(t - \theta_m^l). \quad (10)$$

In practice, the delta function around every estimated eigenvalue $\delta(t - \theta_m^l)$ was replaced by a Gaussian with width σ centered at θ_m^l , i.e., $g_\sigma(t - \theta_m^l)$. This can be understood intuitively as regularizing the spectrum by smoothing it with a Gaussian kernel. A heuristic for setting σ was given in [9]. We summarize FASTLANCZOS in Algorithm 2 and LANCZOSAPPROXSPEC in Algorithm 3.

2.4. Complexity of FASTLANCZOS

Each of the M iterations requires a single Hessian-vector multiplication. As previously mentioned, this product requires $O(n_{\text{train}}p)$ complexity. The total runtime complexity of the algorithm is therefore $O(Mn_{\text{train}}p)$. As for memory requirements; we only save three vectors and as such the memory complexity is merely $O(p)$.

Algorithm 3: LANCZOSAPPROXSPEC(H, M, K, n_{vec})

Input: Linear operator $H \in \mathbb{R}^{p \times p}$ with spectrum in the range $[-1, 1]$.
Number of iterations M .
Number of points K .
Number of repetitions n_{vec} .

Result: Density of the spectrum of H evaluated at K evenly distributed points in the range $[-1, 1]$.

for $l = 1, \dots, n_{\text{vec}}$ **do**

$\{\theta_m^l\}_{m=1}^M, \{y_m^l\}_{m=1}^M = \text{FASTLANCZOS}(H, M)$;

end

$\{t_k\}_{k=1}^K = \text{linspace}(-1, 1, K)$;

for $k = 1, \dots, K$ **do**

$\sigma = \frac{2}{(M-1)\sqrt{8 \log(1.25)}}$;

$\phi_k = \frac{1}{n_{\text{vec}}} \sum_{l=1}^{n_{\text{vec}}} \sum_{m=1}^M y_m^l [1]^2 g_\sigma(t - \theta_m^l)$

end

return $\{\phi_k\}_{k=1}^K$;

2.5. Instability

It can be proved that, under exact arithmetic, the Lanczos algorithm constructs an orthonormal basis. However, in practice the calculations are performed in floating point arithmetic, resulting in loss of accuracy and orthogonality. This is why the reorthogonalization step in Algorithm 1 was introduced in the first place. From our experience, we did not find the lack of reorthogonalization to be an issue, except for an occasional failure in computing the eigendecomposition of the tridiagonal matrix.

2.6. NORMALIZATION

As a side note, the first step in approximating the spectrum of a large matrix is to renormalize its range to $[-1, 1]$. This can be done using any method that allows to approximate the maximal and minimal eigenvalue of a matrix – for example, the power method. In this work we follow the method proposed in [10]. We summarize the procedure in Algorithm 4.

2.7. Reproducible research

The authors of [10] provided implementations for many of the spectrum approximation methods they proposed, including Lanczos, which is our method of choice. However, since the code was written in C and would not allow for GPU acceleration, we decided to re-implement the method in the deep learning framework PyTorch. We plan to release the implementations of NORMALIZATION, FASTLANCZOS, LANCZOSAPPROXSPEC, LOWRANKDEFLECTION, KPM and other related methods with the publication of this paper.

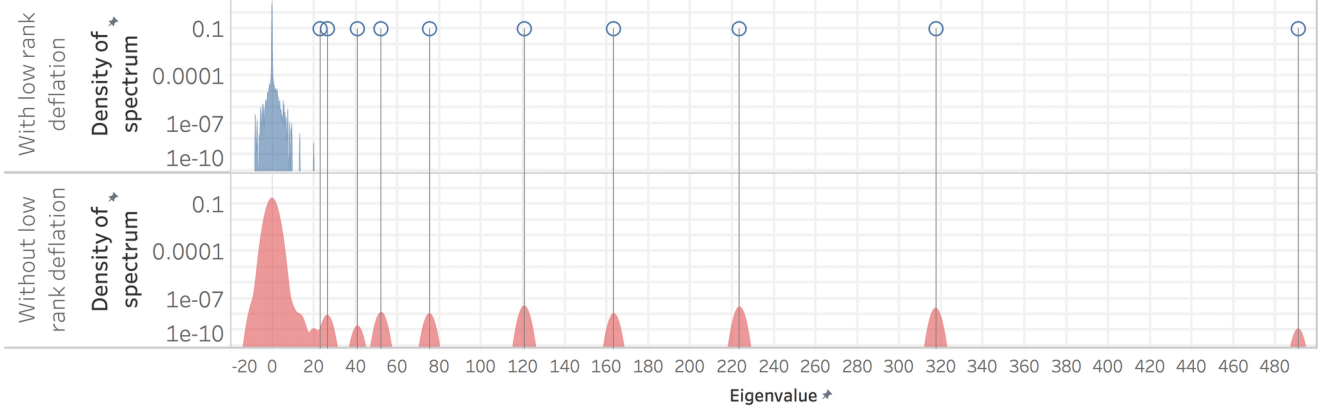


Figure 3: *Benefits of low rank deflation.* Spectrum of the train Hessian for ResNet18 trained on MNIST with 136 examples per class. Top panel: LOWRANKDEFLATION followed by LANCZOSAPPROXSPEC. Bottom panel: LANCZOSAPPROXSPEC only. Notice how the top eigenvalues at the top panel align with the outliers in the bottom panel. Using low rank deflation allows for precise detection of outlier location and improved ‘resolution’ of the bulk distribution.

Algorithm 4: NORMALIZATION (H, M_0, κ)

Input: Linear operator $H \in \mathbb{R}^{p \times p}$.
Number of iterations M_0 .
Margin percentage κ .
Result: Linear operator $H \in \mathbb{R}^{p \times p}$ with spectrum in the range $[-1, 1]$.
 $\{\theta_m\}_{m=1}^{M_0}, \{y_m\}_{m=1}^{M_0} = \text{FASTLANCZOS}(H, M_0)$;
 $\lambda_{\min} = \theta_1 - \|(H - \theta_1 I)y_1\|$;
 $\lambda_{\max} = \theta_{M_0} + \|(H - \theta_{M_0} I)y_{M_0}\|$;
 $\Delta = \kappa(\lambda_{\max} - \lambda_{\min})$;
 $\lambda_{\min} = \lambda_{\min} - \Delta$;
 $\lambda_{\max} = \lambda_{\max} + \Delta$;
 $c = \frac{\lambda_{\min} + \lambda_{\max}}{2}$;
 $d = \frac{\lambda_{\max} - \lambda_{\min}}{2}$;
return $\frac{H - cI}{d}$;

2.8. LOWRANKDEFLATION

As Figures 1 and 2 show, the spectrum of the Hessian follows a bulk-and-outliers structure. Moreover, the number of outliers is often equal to C , the number of classes in the classification problem. It is therefore natural to extract the top C outliers using, for example, the QR algorithm, and then to apply LANCZOSAPPROXSPEC on a rank C deflated operator to approximate the bulk. This allows for an improved detection of outlier location and for improved approximation of the bulk. The latter can be explained as follows: approximating the subset of the spectrum that contains the bulk only is simpler than approximating the whole spectrum, which contains both the bulk and the outliers. We demonstrate the benefits of LOWRANKDEFLATION in Figure 3 and summarize its steps in Algorithm 5.

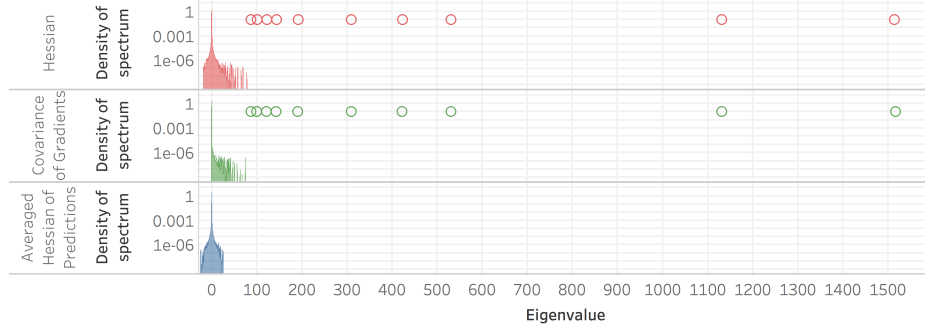
Algorithm 5: LOWRANKDEFLATION (H, C, T)

Input: Linear operator $H \in \mathbb{R}^{p \times p}$.
Rank of deflation C .
Number of iterations T .
Result: Approximate eigenvalues $\{\lambda_c\}_{c=1}^C$.
Approximate eigenvectors $\{v_c\}_{c=1}^C$.
for $c = 1, \dots, C$ **do**
 sample $v_c \sim \mathcal{N}(0, I)$;
 $v_c = \frac{v_c}{\|v_c\|_2}$;
end
 $Q = \text{QR}(V)$;
for $t = 1, \dots, T$ **do**
 $V = HQ$;
 $Q = \text{QR}(V)$;
end
for $c = 1, \dots, C$ **do**
 $\lambda_c = \|v_c\|_2$
end
return $\{\lambda_c\}_{c=1}^C, \{v_c\}_{c=1}^C$

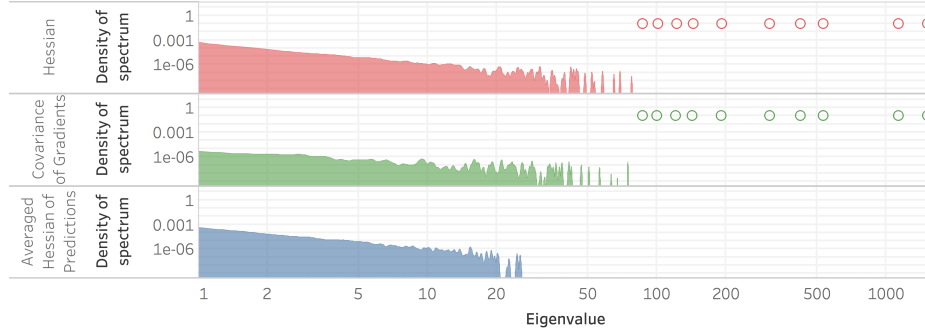
3. Experiments

3.1. Training the networks

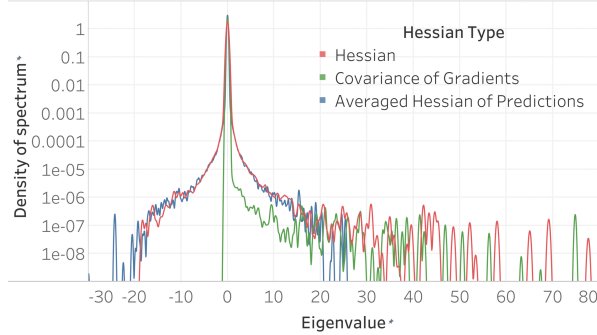
We present here results from training the VGG11 and ResNet18 architectures on MNIST, Fashion MNIST, CIFAR10 and CIFAR100 datasets. We use stochastic gradient descent with momentum 0.9, batch size 128 and weight decay 5×10^{-4} . The learning rate was decreased by a factor of 10 at 1/3 and 2/3 of the total amount of epochs. For each combination of dataset and architecture, we pick the best initial learning rate in terms of test classification performance and then approximate the spectrum of the Hessians



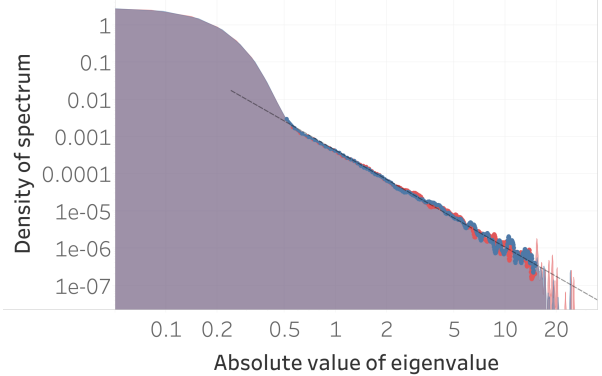
(a) *Outlier attribution.* Top panel: spectrum of Hessian. Middle panel: spectrum of covariance of gradients. Bottom panel: spectrum of averaged Hessian of predictions. Note that the outliers that are present in the top panel are also present, at the same locations, in the middle panel, but not present at all in the lower panel. This indicates that the outliers that have been observed in the Hessian are attributable to the covariance of gradients component.



(b) *Attribution of bulk.* The above plot with logarithmic scale on the x-axis (negative x-axis range omitted). Note the y-axis scales and the vertical height of the bulk. In particular note that the vertical height of the bulk is comparable for the top and bottom panels but not for the middle panel, which is much smaller. This indicates that the bulk of the spectrum originates from the averaged Hessian of predictions.



(c) *Attribution of bulk.* Zoom in on the bulks of the Hessian and its two components. Note the strong correlation between the spectrum of the Hessian and the averaged Hessian of predictions in the range $[-20, 20]$. This indicates that the bulk originates, for the most part, from the averaged Hessian of predictions. Note that the upper tail of the Hessian and covariance of gradients obey eigenvalue interlacing, as in Cauchy interlacing theorem.



(d) *Tail properties of averaged Hessian of predictions.* The x-axis is on a logarithmic scale. The positive eigenvalues of the averaged Hessian of predictions are plotted in red and the absolute value of the negative ones in blue. The spectrum of the averaged Hessian of predictions is almost perfectly symmetric about the origin. Fitting a power law trend (which appears linear on a log-log scale) on part of the spectrum results in a fit $\phi = 4.3 \times 10^{-4} |\lambda|^{-2.6}$ with an R^2 of 0.98. This implies that the distribution of the eigenvalues can not be Wigner's semicircle law, nor other classical random matrix theory distributions.

Figure 4: Spectrum of the test Hessian with its constituent components for VGG11 trained on MNIST sub-sampled to 2599 examples per class. For the test Hessian and the covariance of gradients component we apply LOWRANKDEFLATION.

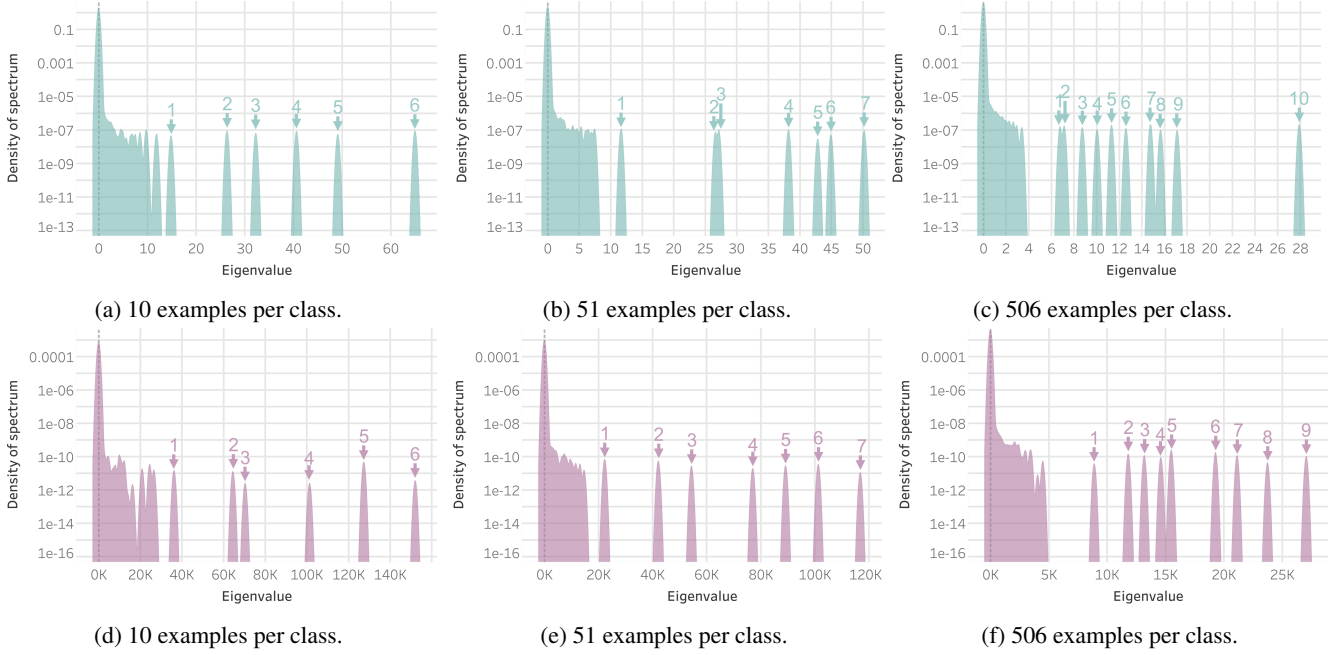


Figure 5: VGG11 trained on CIFAR10 for various sample sizes. On the **top** panel we observe the covariance of gradients of the **train** Hessian. On the **bottom** panel we observe the covariance of gradients of the **test** Hessian. In both train and test, as the sample size increases, more outliers emerge from the bulk.

Dataset	MNIST	Fashion	CIFAR10	CIFAR100
Learning rate	0.1	0.1	0.25	0.25
	0.075	0.075	0.1	0.1
	0.05	0.05	0.075	0.075
	0.025	0.025	0.05	0.05
	0.01	0.01	0.025	0.025
			0.0075	0.0075
Epochs	200	200	350	350

Table 1: Summary of experiment parameters.

on that model alone.

We are interested in investigating the behaviour of the outliers and the bulk as function of the sample size. As such, we sub-sampled (without replacement) the datasets for different amounts of examples per class and repeated for each sample size the experiments above. We summarize the experimental setting in Table 1.

3.2. Spectrum of the Hessian

We are interested in spectra deriving from these choices

$$\{\text{train, test}\} \times \{\text{Hessian,} \quad (11)$$

covariance of gradients,
averaged Hessian of predictions}.

For each operator H , we begin by computing $\text{NORMALIZATION}(H, M_0=64, \kappa=0.05)$. Optionally, we then apply $\text{LOWRANKDEFLATION}(H, C, T=256)$. Finally we approximate the spectrum using $\text{LANCZOSAPPROXSPEC}(H, M=256, K=1024, n_{vec}=1)$.

Due to space limitations, we show only a subset of our results and publish the remaining data and code online to allow other researchers to explore our results further. We summarize our findings in Figures 1, 2, 3, 4 and 5. In all our plots we denormalize the spectrum into its original range (which is not $[-1, 1]$). We provide our interpretations of the results in the captions of the figures.

4. Conclusion

This work studied modern deepnet Hessians at the full scale used in recent contest-winning entries and in serious applications. It shows that the bulk-and-outliers structure previously observed in small scale networks is also visible in full scale networks. It gives novel decompositions and novel attributions using more solid methods than previously and identifies new patterns and phenomena in the eigenvalues of the Hessian.

References

- [1] Z. Bai and J. Yao. On sample eigenvalues in a generalized spiked population model. *Journal of Multivariate Analysis*, 106:167–177, 2012. 2
- [2] J. Baik, G. B. Arous, S. Péché, et al. Phase transition of the largest eigenvalue for nonnull complex sample covariance matrices. *The Annals of Probability*, 33(5):1643–1697, 2005. 1
- [3] J. Baik and J. W. Silverstein. Eigenvalues of large sample covariance matrices of spiked population models. *Journal of multivariate analysis*, 97(6):1382–1408, 2006. 1
- [4] D. A. Drabold and O. F. Sankey. Maximum entropy approach for linear scaling in the electronic structure problem. *Physical review letters*, 70(23):3631, 1993. 4
- [5] F. Ducastelle and F. Cyrot-Lackmann. Moments developments and their application to the electronic charge distribution of d bands. *Journal of physics and chemistry of solids*, 31(6):1295–1306, 1970. 4
- [6] K. He, X. Zhang, S. Ren, and J. Sun. Deep residual learning for image recognition. In *Proceedings of the IEEE conference on computer vision and pattern recognition*, pages 770–778, 2016. 2
- [7] I. M. Johnstone. On the distribution of the largest eigenvalue in principal components analysis. *Annals of statistics*, pages 295–327, 2001. 1, 2
- [8] C. Lanczos. *An iteration method for the solution of the eigenvalue problem of linear differential and integral operators*. United States Governm. Press Office Los Angeles, CA, 1950. 4
- [9] R. Li, Y. Xi, L. Erlandson, and Y. Saad. The Eigenvalues Slicing Library (EVSL): Algorithms, Implementation, and Software. 5
- [10] L. Lin, Y. Saad, and C. Yang. Approximating spectral densities of large matrices. *SIAM review*, 58(1):34–65, 2016. 4, 5
- [11] V. A. Marcenko and L. A. Pastur. Distribution of eigenvalues for some sets of random matrices. *Mathematics of the USSR-Sbornik*, 1(4):457, 1967. 1
- [12] C. H. Martin and M. W. Mahoney. Implicit self-regularization in deep neural networks: Evidence from random matrix theory and implications for learning. *arXiv preprint arXiv:1810.01075*, 2018. 3
- [13] D. Paul. Asymptotics of sample eigenstructure for a large dimensional spiked covariance model. *Statistica Sinica*, pages 1617–1642, 2007. 1
- [14] L. Sagun, L. Bottou, and Y. LeCun. Eigenvalues of the hessian in deep learning: Singularity and beyond. *arXiv preprint arXiv:1611.07476*, 2016. 1, 2
- [15] L. Sagun, U. Evci, V. U. Guney, Y. Dauphin, and L. Bottou. Empirical analysis of the hessian of over-parametrized neural networks. *arXiv preprint arXiv:1706.04454*, 2017. 1, 2
- [16] K. Simonyan and A. Zisserman. Very deep convolutional networks for large-scale image recognition. *arXiv preprint arXiv:1409.1556*, 2014. 2
- [17] I. Turek. A maximum-entropy approach to the density of states within the recursion method. *Journal of Physics C: Solid State Physics*, 21(17):3251, 1988. 4
- [18] J. C. Wheeler and C. Blumstein. Modified moments for harmonic solids. *Physical Review B*, 6(12):4380, 1972. 4